



Universidad Autónoma
de Madrid

Biblos-e Archivo
Repositorio Institucional UAM

Repositorio Institucional de la Universidad Autónoma de Madrid

<https://repositorio.uam.es>

Esta es la **versión de autor** del artículo publicado en:

This is an **author produced version** of a paper published in:

Intelligence 68 (2018): 21 – 29

DOI: <https://doi.org/10.1016/j.intell.2018.02.006>

Copyright: © 2018 Elsevier Inc. This manuscript version is made available under the CC-BY-NC-ND 4.0 licence <http://creativecommons.org/licenses/by-nc-nd/4.0/>

El acceso a la versión del editor puede requerir la suscripción del recurso

Access to the published version may require subscription

Brain-intelligence relationships across childhood and adolescence: A latent-variable approach

Francisco J. Román¹, Daniel Morillo¹, Eduardo Estrada², Sergio Escorial³,
Sherif Karama⁴, Roberto Colom^{1*},

(1) Universidad Autónoma de Madrid, Madrid (Spain).

(2) Department of Psychology, University of California at Davis, Davis (USA).

(3) Universidad Complutense de Madrid, Madrid (Spain).

(4) Montreal Neurological Institute (MNI), McGill University, Montreal (Canada).

** Corresponding author:*

Roberto Colom

Universidad Autónoma de Madrid

28049 Madrid (Spain)

Voice: 91 497 41 14

Email: roberto.colom@uam.es

Highlights

- Longitudinal changes in g are related with developmental cortical changes
- Longitudinal latent variable analyses revealed an increase in g scores
- Older individuals showed greater cortical decrease along with smaller intelligence increase
- Thickness preservation in brighter individuals was observed at early adolescence

Abstract

The analysis of the relationships between cortical and intellectual development is a complex matter. Greater brain plasticity in brighter individuals has been suggested, but the associations between developmental cortical changes and variations in the general factor of intelligence (g) across time at the latent level have not been addressed. For filling this gap, here we relate longitudinal changes in g with developmental changes in cortical thickness and cortical surface area. One hundred and thirty-two children and adolescents representative of the population from the Pediatric MRI Data Repository completed the Wechsler Abbreviated Scale of Intelligence in three time points and MRI scans were also obtained (mean inter-registration interval ≈ 2 yrs., age range = 6.1 to 21.3 yrs.). Longitudinal latent variable analyses revealed an increase in g scores amounting to a full standard deviation on average. Intelligence differences estimated at the latent level were significantly correlated related with cortical changes. Older individuals showed greater decrease in cortical values along with smaller increase in intelligence. Furthermore, thickness preservation in brighter individuals was observed at early adolescence (10-14 years).

Keywords. Intellectual development; General factor of intelligence (g); Cortical development; Cortical thickness; Cortical surface area

1. INTRODUCTION

The study of the relationship between age changes in general cognitive ability (g) and brain maturation deserves investigation (Johnson, 2013). There are acknowledged changes in cognitive and cortical features during childhood and adolescence, and, therefore, the relationships between differences in brain structure and cognition may change across age (Van Petten, 2004).

Research has shown average cortical thinning in childhood and early adolescence (Sowell et al., 2003, 2007, age range: 5 to 11 years), along with average cortical surface area expansions in adolescence (Schnack et al., 2014, age range: 9 to 60 years). Non-linear cortical thinning has been revealed after studying children (6 to 10 years), adolescents (10 to 20 years), and adults (20 to 30 years) (Zhou et al., 2015): accelerated thinning was observed during adolescence and cortical surface area increased similarly with age in children and adolescents (although findings are not entirely consistent, see Alemán-Gómez et al., 2013).

Zhou et al. (2015) failed to find relationships between changes in thickness and surface area studying the same sample of individuals: age changes in both cortical indices were not coordinated. Raznahan et al. (2011, age range: 6 to 22 years) computed the annual percent of change for thickness and surface area finding similar results for both indices across ages, although boys showed higher percentages of surface area changes than girls from 6 to 14 years. Afterwards, girls and boys showed similar percentages of change.

Zhou et al. (2015) underscored the large consistency across studies regarding cortical thinning during development. However, their results were heterogeneous: some

individuals did show thinning, some others did show thickening, and some hardly showed any change.

These developmental cortical differences at the individual level were also observed by Burgaleta et al. (2014) who analyzed their relationship with cognitive ability changes – also at the individual level—as assessed by WASI IQ scaled scores. Their results revealed that participants showing IQ gains over time were characterized by cortical thickness preservation, whereas those showing greater cortical thinning lost IQ points over time. Therefore, IQ changes were associated with the dynamics of cortical thickness across development. However, Burgaleta et al. (2014) failed to find any substantial relationship between changes in cortical surface area (showing both expansion and contraction) and IQ changes.

On the other hand, Schnack et al. (2014) analyzed five age groups [below 12 years (N = 114), between 12 and 20 years (N = 76), between 20 and 30 years (N = 152), between 30 and 40 years (N = 105), and above 40 years (N = 57)] finding relationships between intelligence assessed at baseline and cortical changes (in thickness and surface area) and concluding that the human brain shows systematic “*intelligence-dependent development*”: brightest children did show thinner cortices than less intelligent children, and faster thinning over time was observed for the former. However, this trend reversed in adulthood: thicker cortices were associated with higher intelligence scores. With respect to cortical surface area, brightest children did show larger values. Surface area expansion approached asymptotic levels during adolescence. High intelligence individuals stopped their cortical expansion at early ages, and, afterwards, decreases were

shown at faster rates. In short, intelligence assessed at baseline was related with the magnitude and time of the life span at which the brain seems to show structural changes.

Schnack et al. (2014) considered intelligence at baseline only, and therefore, relationships between changes in cortical indices and intellectual changes across development were not addressed. Nevertheless, cortical-intelligence relationships might change across development. Thus, for instance, the study by Koenis et al. (2015, age range: 9 to 15 years) revealed substantial relationships between changes in the organization of structural brain networks and intellectual functioning: better local efficiency in temporal and frontal regions were related to higher intelligence scores. Individual development of intelligence seems to be coordinated with individual development of brain structural networks.

Here we study the relationships between cortical development and intellectual ability across childhood and adolescence. We pursue this main goal analyzing intellectual changes by applying longitudinal structural equation modeling (Estrada et al., 2015, Widaman, Ferrer, & Conger, 2010). Developmental changes in general cognitive ability (g) will be modeled at the latent level. Afterwards, changes in intelligence will be related with changes in cortical thickness and cortical surface area. Psychological and biological data were obtained from one hundred and thirty two children and adolescents at three time points separated by approx. two years each.

To our knowledge, a latent variable approach has not been applied before. A common procedure is to compute full-scale IQ scores based on the raw values obtained from the tests of a given measurement battery, and then age-norming them (e.g. computing IQ scores from the WISC). This procedure assumes that a) all the tests share the same

percentage of variance with the common factor, and b) there is no measurement error. Instead of using scaled scores for intelligence at each measurement occasion, here we model the scores in a latent factor representing general intelligence (*g*). This allows computing error-free estimates of intelligence, as well as cleaner estimates of between individual differences and within individual changes over time (Barbey et al., 2012, Colom et al., 2009, 2013, Estrada et al., 2015, Gläscher et al., 2010, Haier et al., 2009, Román et al., 2014).

Because we obtained measures across childhood and adolescence, mental abilities –as well as other variables such as height or physical abilities– are expected to increase. Consider height as an example: any normative sample will increase in height between 6 and 21 years of age. Therefore, a very high correlation is expected between height and age. Computing age-normed scores of age controls for this correlation, but this approach would hide the fact that individuals are taller at *t*₃ than at *t*₁. The same problem arises for intelligence. The latent variable approach applied here allows overcoming this situation by capturing the growth in *g* while being unaffected by the high collinearity between *g* and age.

2. METHOD

2.1. Participants

132 children and adolescents (74 girls, 56.1%) representative of the U.S. population (2000 Census data) from the Pediatric MRI Data Repository created for the National Institute of Mental Health MRI Study of Normal Brain Development (Evans & The Brain Development Cooperative Group, 2006) were analyzed (age range: 6.1 – 21.3; mean age

at time 1 = 10.92, SD = 3.13). They were scanned at three time points (the mean inter-scan interval was ≈ 2 yrs.). Only participants without prior history of psychiatric disorders, neurological, or other medical illnesses with central nervous system implications were selected. Also, all MRI scans analyzed here passed strict quality control (QC). Figure 1 shows the timeline of the present study.

PLEASE INSERT FIGURE 1 AROUND HERE

2.2. Cognitive Measures

Intelligence was assessed with The Wechsler Abbreviated Scale of Intelligence (WASI) (Wechsler, 1999). Vocabulary, Similarities, Matrix Reasoning, and Block Design are the tests included in this battery, and they were administered at the three time points considered (Figure 1). These tests were analyzed for modeling changes in the general factor of intelligence (g) across time points (t) –please see below for further details.

2.3. MRI acquisition

For the structural images analyzed here, a high-resolution 3D T1-weighted Spoiled Gradient Recalled (SPGR) echo sequence was applied. 1 mm isotropic data were acquired sagittally (whole head); TR = 22–25 ms, TE = 10–11 ms. Excitation pulse = 30°, refocusing pulse = 180°. FOV = AP 256 mm, LR 160–180 mm. Matrix size = AP 256 mm, LR for 1 mm isotropic. Slice thickness of ~ 1.5 mm for GE scanners (with a limit of 124 slices) was allowed to guarantee whole head coverage.

2.4. Surface-Based Morphometry

MRIs were processed through the CIVET pipeline (version 1.1.9) (Ad-Dab'bagh et al., 2006; Kim et al., 2005; MacDonald et al., 2000) for obtaining measures of regional cortical thickness (CT) and cortical surface area (CSA). Specific stages for the analyses were: (1) linear registration (12-parameter) to MNI-Talairach (*ICBM152*) space, (2) images corrected for radio-frequency non-uniformities and a brain mask computed, (3) tissue classification into white matter (WM), gray matter (GM), and cerebrospinal fluid (CSF), (4) generation of high-resolution hemispheric surfaces with 40,962 vertices each, (5) registration of surfaces to a high-resolution template, (6) cortical thickness is computed by evaluating the distance, in mm, between the original WM and GM surfaces transformed back to the native space of the original MR images, then interpolated onto the surface template, (7) vertex-based areas computed directly on the resampled surfaces and measure local variations of area/volume contraction and expansion relative to the vertex distribution on the surface template, (8) smoothing using a 20-mm kernel for CT and 40-mm for CSA. More information regarding these steps can be found in Karama et al. (2009).

2.5. Analyses

2.5.1. Changes in general intelligence (g)

For analyzing age changes in general intelligence (*g*) at the latent level, we computed longitudinal factorial invariance analyses. This technique evaluates whether the same latent construct is measured by a set of indicators (measures) at different time points (*t*), and whether the relationships between the latent variable and the indicators remain invariant across time points (Meredith, 1993; Meredith & Horn, 2001; Widaman, Ferrer,

& Conger, 2010). It is particularly applicable when a set of indicators is available for measuring the same latent construct and the sample size is adequate. Our dataset meets both requirements. Note that it is crucial to show that the same construct of interest is measured across time points, and, therefore, theoretically substantive comparisons can be made (Estrada et al., 2015).

For assessing factorial invariance, a set of nested structural equation models with increased invariance restrictions are usually specified. The fit of the less restricted model (configural invariance) is examined first and more constrained versions are considered in successive steps. We compared a series of nested models with increased levels of invariance across time points. The analyses were carried out in Mplus 7 (Muthén & Muthén, 1998, 2015) with maximum likelihood estimation. The structural equation model used for the invariance tests is shown in Figure 2.

PLEASE INSERT FIGURE 2 AROUND HERE

2.5.1.1. Baseline Model

We adapted here the notation proposed by McArdle (1988) and Widaman, Ferrer and Conger (2010). The observed variables are represented as squares, the latent variables as circles, and the constant unit (for computing means and intercepts) as a triangle. The arrows from the constant to the latent variables (α_1 , α_2 and α_3) represent latent variable intercepts, whereas the arrows from the constant to the observed variables (τ_{11} to τ_{34}) represent observed variables intercepts. The arrows from the latent variables to their respective observed indicators (λ_{11} to λ_{34}) represent factor loadings.

The latent factor metric is defined by fixing its variance to one at every measurement occasion ($\sigma_{11}^2 = \sigma_{22}^2 = \sigma_{33}^2 = 1$), and fixing the latent means $\alpha_1 = \alpha_2 = \alpha_3 = 0$. The covariances between the latent variables are represented by σ_{12} , σ_{13} and σ_{23} . The latent factor g is regressed on the age at the three measurement occasions (γ_{11} , γ_{22} and γ_{33}). The unique variance for each observed indicator is represented by θ_{11} to θ_{34} . Covariances between observed indicators across measures (not depicted in Figure 2) are allowed in order to account for correlations between test-specific variance over time. If the baseline model shows adequate fit, *configural* factorial invariance holds. This entails that variances, covariances, and means of the observed variables are adequately represented by the structural equation model.

2.5.1.2. Evaluating invariance across measures and times

Starting with Model 1, we fitted a series of models with increased restrictions for assessing specific hypothesis about the data. This series is consistent with the procedure for evaluating factorial invariance proposed by Widaman and Reise (1997) and Widaman, Ferrer and Conger (2010). Besides, it introduces one final step for formally testing hypothesis regarding equal influence of the age on g across measurements.

In Model 2, factor loadings are constrained to be equal across measurements ($\lambda_{11} = \lambda_{21} = \lambda_{31}$, $\lambda_{12} = \lambda_{22} = \lambda_{32}$, $\lambda_{13} = \lambda_{23} = \lambda_{33}$, $\lambda_{14} = \lambda_{24} = \lambda_{34}$). If this model shows adequate fit, *weak* factorial invariance holds. This entails that the pattern of variances-covariances for the observed variables, and the weight of g on each of them, can be assumed as constant across measurements.

In Model 3, the intercepts are constrained to be equal across measurements ($\tau_{11} = \tau_{21} = \tau_{31}$, $\tau_{12} = \tau_{22} = \tau_{32}$, $\tau_{13} = \tau_{23} = \tau_{33}$, $\tau_{14} = \tau_{24} = \tau_{34}$), whereas the intercepts of g is fixed at $t1$ ($\alpha_1 = 0$) and freely estimated at the remaining time points (α_2 and α_3). If this model shows adequate fit, *strong* factorial invariance holds. Note that the indicators' mean scores are not supposed to be equal across time, since participants are expected to achieve a higher performance as a consequence of maturation. Hence, by freely estimating α_2 and α_3 , the model allows testing whether the observed changes in the indicators are explained uniquely by changes in the latent variable g .

In Model 4, the residual variances are constrained to be equal across the three measurements ($\theta_{11} = \theta_{21} = \theta_{31}$, $\theta_{12} = \theta_{22} = \theta_{32}$, $\theta_{13} = \theta_{23} = \theta_{33}$, $\theta_{14} = \theta_{24} = \theta_{34}$). If this model shows adequate fit, *strict* factorial invariance holds. This entails that the unique variance of the observed variables (not explained by g) is constant across measurements. This is the highest possible level of factorial invariance.

In addition to the standard factorial invariance testing procedure, we fitted Model 5 for testing whether the regression weight of Age on g can be assumed to be constant across time points ($\gamma_{11} = \gamma_{22} = \gamma_{33}$). If this model shows adequate fit, the impact of age on g is constant across measurements.

2.5.1.3. Model fit

Each model is a constrained version of the previous one. Hence, they are nested models and thus can be evaluated with likelihood ratio χ^2 difference tests for comparing fit differences across models. We also computed the root mean square of approximation,

RMSEA (Browne & Cudeck, 1993), the comparative fit index, *CFI* (Bentler, 1990), and the Tucker-Lewis index, *TLI* (Tucker & Lewis, 1973).

For *RMSEA*, values between 0 and .06 indicate very good fit, values between .06 and .08 indicate reasonable fit, and values greater than .10 indicate poor fit. For *CFI* and *TLI* indices, acceptable values must be larger than .90 and excellent values must be above .95 (Schreiber, Nora, Stage, Barlow, & King, 2006; Schweizer, 2010).

2.5.2. Neuroimaging analyses

2.5.2.1. Brain-intelligence correlations

Developmental cortical changes in thickness (CT) and surface area (CSA) were computed for the entire cortex and plotted along with the calculated longitudinal latent intellectual changes across age. Afterwards, we calculated the correlation between these cortical and intellectual values across age.

2.5.2.2. Linear mixed-model regression analyses

Using SurfStat, linear mixed-model regression analyses were computed using all scans and all *g* measures for each cortical index (CT and CSA) at the vertex level. Age and *g* values were centered variables. Because this is a multi-center study, the models included ‘scanner number’ as a categorical control variable (*scan*) (see Ducharme et al., 2016):

$$M = I + g + Age + Age^2 + Age^3 + Age \times g + Age^2 \times g + Age^3 \times g + random(Subject) + scan + I$$

[Equation 1]

where $1 = \beta_0$ term in a regression model which is forced to be 1 here, and I = the identity matrix, which allows for independent ‘white’ noise in every observation.

CT and CSA values were the dependent variables. The interaction Age x g for predicting CT and CSA indices will be reported. The original model was simplified deleting the terms failing to pass statistical significance. Specifically, here the linear and cubic interactions were not significant. Therefore, this was the final model analyzed:

$$M = I + g + Age + Age^2 + Age \times g + Age^2 \times g + random(Subject) + scan + I.$$

[Equation 2]

Non-significant terms were excluded for simplifying the model. However, we computed again the analyses using the full model ($M = I + g + Age + Age^2 + Age^3 + Age \times g + Age^2 \times g + Age^3 \times g + random(Subject) + scan + I$) and results for the square effects were the same. Only cubic interactions were removed from the final model.

The threshold for the statistical maps was $q = 0.05$ corrected for multiple comparisons (family wise error rate below 5%).

2.5.2.3. Relative change rate (RCR)

Following Schnack et al.’s (2014) approach, relative change rates (RCRs) were computed for exploring further the relationship between cortical changes and intellectual development. Instead of the whole cortex, we used the vertices where the interaction term was statistically significant after the computed linear mixed-model regression analyses

(age² x g). For each participant, RCRs were computed with measures obtained in *t1* and *t3*. Afterwards, a locally weighted regression (loess) (Cleveland & Devlin, 1988) model was fit using each RCR as criteria. This procedure was implemented in the R package *stats* by the function *loess*.

We used two predictors to fit these models: mean age (between *t1* and *t3* measures) was used as a locally weighted predictor. Previous evidence has shown that intelligent increments across time follow a quadratic law in childhood and early adolescence (Salthouse, 2017, Shaw et al., 2006). Therefore, the residual of the quadratic regression of *g* on age was computed as a linear predictor, so a slope parameter (*b*) was obtained for each value of age. We used a tricube weight function (Cleveland & Devlin, 1988) for the locally weighted predictor (mean age). The span parameter (fraction of points in the neighborhood) was equal to .5.

To compute the parametric predictor, *g* was previously standardized for *t1* (and the values in *t2* and *t3* appropriately rescaled). Then, a linear mixed quadratic regression model of *g* on age was computed, with both a first and second order terms on age, and a random effect term for the measure (*t1* to *t3*). Finally, the residuals at the three measures were averaged (Cronbach's $\alpha = .997$) as an estimator of *g* for each participant.

To obtain an estimate of the significance of the slope (*b*) parameters for each age, the values of the residual of *g* were permuted and the model computed again 2,000 times, thus obtaining a null distribution of *b* as suggested by Schnack et al. (2014).

3. RESULTS

3.1. Latent intelligence across time points

Table 1 reports the fit from each tested model and it includes the likelihood ratio difference tests between successive models.

PLEASE INSERT TABLE 1 AROUND HERE

The goodness of fit for Model 1 indicates that the hypothesized model adequately describes the data.

When all the factor loadings are restricted to be equal across measures (Model 2a), the misfit increases statistically ($\Delta\chi^2 / \Delta df = 50.6/8, p < .001, \Delta CFI = .020, \Delta TLI = .023, \Delta RMSEA = -.021$). Therefore, full weak factorial invariance does not hold. However, when the factor loadings for the Matrices test is allowed to be different across time, whereas the rest of factor loadings are constrained to be equal (Model 2b), the misfit increases statistically ($\Delta\chi^2 / \Delta df = 18.4/6, p = .005$) but the rest of fit indices do not increase substantially, or even decrease ($\Delta CFI = .006, \Delta TLI = .005, \Delta RMSEA = -.005$). Therefore, partial weak invariance can be assumed (Widaman et al., 2010). This implies that the relative weight of the latent factor on the Block, Similarities and Vocabulary tests does not change across time (t), whereas it does change for the Matrices test. Given that the latent factor can be adequately estimated with three observed indicators, and the longitudinal differences in the Matrices test are theoretically expected, we decided to consider only partial invariance in the remaining models.

When the intercepts of the observed indicators are restricted to be equal across time points, and the latent variable intercepts (α_2 and α_3) are freely estimated for t_2 and t_3 (Model 3), the misfit does not increase statistically ($\Delta\chi^2 / \Delta df = 8.1/4, p = .087$; $\Delta CFI = .002$, $\Delta TLI = .001$, $\Delta RMSEA = .000$). Consequently, the changes at the tests' level are properly explained by the net change in the underlying latent variable (g).

When the residual variances of the observed indicators are restricted to be equal at the three measurements, (Model 4), the misfit suffers a minimal but statistically significant increase ($\Delta\chi^2 / \Delta df = 16.2/6, p = .013$; $\Delta CFI = .005$, $\Delta TLI = .003$, $\Delta RMSEA = -.003$). Since the substantive importance of the change in the model's fit is very small, strict factorial invariance holds. This implies that the proportion of variance of the observed indicators, which is not explained by the latent factor, is constant across measurements.

Finally, when the regression weights of age on g are constrained to be equal at the three time points (Model 5), the misfit suffers a large and statistically significant increase ($\Delta\chi^2 / \Delta df = 136.6/2, p < .001$; $\Delta CFI = .065$, $\Delta TLI = .073$, $\Delta RMSEA = -.052$). The standardized regression weights estimated by the model were $\gamma_{11} = .90$ at t_1 (unstandardized $\gamma_{11} = .62$), $\gamma_{22} = .82$ at t_2 (unstandardized $\gamma_{22} = .46$) and $\gamma_{33} = .70$ at t_3 (unstandardized $\gamma_{33} = .33$). This implies that the age impact on g changes over time. For corroborating this result, we compared the regression weights of Model 4 for detecting significant pair differences among them. The results of these pair comparisons are reported in Table 2. The pair comparisons show that all the regression weights are different among them.

PLEASE INSERT TABLE 2 AROUND HERE

3.2. *Changes in general intelligence (g)*

Mean g values at different time points were computed for evaluating maturational changes using the estimates from Model 4. The intercept of the g factor (α_1) at $t1$ was fixed to 0 and estimated freely in $t2$ and $t3$ following the guidelines of the factorial invariance analytic procedure. The mean for each time point was computed as α (intercept of g) + γ (weight of Age on g) * mean age. Results are shown in Table 3.

PLEASE INSERT TABLE 3 AROUND HERE

The mean value for the general factor (g) across time is arbitrary, but the difference obtained in the mean values for g can be interpreted as an effect size. Results showed a value of $d = .60$ for the difference in g from $t1$ to $t2$. This difference was smaller from $t2$ to $t3$ ($d = .48$). Finally, the difference between $t1$ and $t3$ showed a value of $d = .98$.

3.3. *Brain-intelligence relation across age*

Figure 3 (Left Panel) depicts the observed changes at the individual level for cortical thickness (CT), cortical surface area (CSA) and g estimates. Thickness and surface area values were obtained from the entire cortex. One hundred and four cases (79.4%) showed thinning across time. Thickening was observed mostly in younger individuals. The sample was more diverse regarding CSA changes: 77 cases (58.8%) experienced surface area contraction, whereas 54 cases (41.2%) experienced surface area expansion. Finally, generalized longitudinal gains in g scores were observed, as expected. Nevertheless, these

intellectual changes were sharper (red) at younger ages and weaker (blue) at older ages – following a quadratic law, as expected.

PLEASE FIGURE 3 A & B AROUND HERE

These cortical and intellectual changes are summarized in Figure 3 (Right Panel): changes in g scores (which are greater in young individuals) correlate with changes in cortical thickness and cortical surface area. Longitudinal changes in g were significantly related with changes in CT (Pearson's $r = .30, p < .000$; Spearman's $\rho = .28, p = .001$) and in CSA (Pearson's $r = .37, p = .000$; Spearman's $\rho = .41, p = .000$).

3.4. Regression results

The interaction age $\times g$ was computed for both cortical features (CT and CSA). The original model included the cubic term since previous reports found a cubic age \times intelligence interaction (Shaw et al., 2006; Schnack et al., 2014). However, we failed to find a statistically significant effect of cubic and lineal terms for both cortical indices. Instead, we found a robust square effect (age² $\times g$) for CT and CSA. Figure 4 shows the results.

PLEASE FIGURE 4 AROUND HERE

Findings for cortical thickness (**blue**) were widely distributed across the entire cortex in bilateral regions, while for cortical surface area (**green**) the statistically significant results were located in right medial orbitofrontal, left fusiform, superior and middle temporal,

and caudal middle frontal. Results found for CSA in left temporal and frontal regions overlapped (**red**) with those observed for CT.

The significant quadratic interaction between age and intelligence ($\text{age}^2 \times g$) means that brain regions for which the development of CT and CSA follow an inverted U-shaped pattern were modulated by intelligence, while regions with a linear or cubic developmental pattern were not modulated by intelligence. This is further explored in the next section.

3.5. Relative Change Rates (RCRs)

Figure 5 (Top Panel) depicts thickness and surface area developmental trends computed from the vertices where the interaction $\text{age}^2 \times g$ was statistically significant (Figure 4). To render these plots, the prediction axis of the residual of g was transformed back into the g metric (standardized for $t1$) using the coefficients of the quadratic regression model (the intercept computed as the average of the intercepts for $t1$ and $t3$). Figure 5 (Bottom Panel) shows at which ages the slope (b) representing cortical changes is statistically significant with respect to the observed intelligence values.

PLEASE FIGURE 5 AROUND HERE

As shown in Figure 5 (Left Top Panel) cortical thinning is manifested in less intelligent individuals of approximately 10 years of age. For brighter individuals, this thinning process happens only in the late adolescence (17 years of age). However, thinning is statistically associated with intelligence from 10 to 14 years of age (Figure 5, Left Bottom

Panel): individuals with lower intelligence scores in this developmental stage show greater thinning.

Figure 5 (Right Top Panel) shows substantial cortical surface area expansion along the full range of intelligence scores for younger individuals (8 years of age). This expansion stops at 9-10 years of age. Surface contraction is observed at 11 years of age, albeit it seems more pronounced in brighter individuals. Afterwards, surface changes are almost absent. Figure 5 (Right Bottom Panel) shows that all surface area changes observed across the developmental period considered here are independent of the computed intelligence values.

4. DISCUSSION

Here we have analyzed the relationships between cortical and intellectual development in a sample of one hundred and thirty-two children and adolescents representative of the general population. Intelligence and cortical data were obtained at three time points separated by approx. twenty-four months each and within an age range of 15 years (from 6.1 to 21.3) (Figure 1).

4.1. Brain-intelligence relationships across development

Intellectual changes during the considered time period were modeled using a latent variable approach. We demonstrated that general cognitive ability (g) obtained after the latent analysis of the four WASI subtests (block design, matrix reasoning, similarities, and vocabulary) can be meaningfully compared across measurement time points. This approach is hardly considered in neuroimaging research, which mostly relies on observed

measures of intelligence, such as IQ scores (Colom et al., 2010, 2013, Colom & Thompson, 2011, Haier et al., 2009, Román et al., 2014).

Results showed developmental intelligence gains, and therefore, as expected, at the group level participants get smarter across this period of the life span (in the same sense that increases in height observed at these ages; Taki et al., 2012). These intellectual changes were correlated with developmental cortical changes (Figure 3) finding statistically significant correlations both for cortical thickness (CT) and cortical surface area (CSA): older individuals showed greater decrease in cortical values along with smaller increase in intelligence.

Regression analyses showed that the effect of age on CT and CSA is moderated by general intelligence (g): we found a strong square effect ($\text{age}^2 \times g$) for both indices (Figure 4). Therefore, brain structural changes did interact with intelligence values. Specifically, results for CT were observed bilaterally in frontal, temporal, parietal, and occipital regions, whereas findings for CSA were mainly circumscribed to temporal and frontal regions. As shown in Figure 4, the interaction between age and intelligence was circumscribed to brain regions of the left frontal and temporal lobes.

The meta-analysis by Basten et al. (2015), addressing the relationship of structural and functional neuroimaging data with individual differences in intelligence, underscored the relevance of temporal and frontal regions for the structural data. Gray matter variations in the parietal lobe were unrelated with intelligence differences. Therefore, individual differences in the structure of a set of frontal and temporal brain regions were seen as especially relevant when accounting for individual differences in intelligence.

These temporal and frontal areas were also sensitive to adaptive working memory training in the Román et al.'s (2016) study. Cortical changes observed for both gray matter features (thickness and surface area) were mainly circumscribed to the temporal lobe. This study also tested the role of baseline intelligence differences separating participants of the training and control groups over the analyzed changes in the cortical indices of interest. Findings revealed that controls with lower intelligence levels at baseline show substantial thinning, but this was not the case for controls with higher intelligence levels at baseline. Importantly, the training group showed thickness preservation regardless of participants' baseline intelligence levels, which led to conclude that the completed cognitive enhancement program compensates for the effect of low baseline intelligence levels.

The findings reported here, showing significant relationships between age changes in cortical features (thickness and surface area) and general intelligence (*g*) mainly in temporal and frontal brain regions, can be seen as consistent with Basten et al.'s (2015) meta-analytic results, but also with the effects of short-term cognitive training over individuals showing substantial differences in their intelligence levels (Román et al., 2016). Cortical structural features within the frontal and temporal lobes seem particularly relevant when accounting for intelligence differences.

4.2. Relative Change Rates

Based on the above findings, we moved one step further building developmental maps based on relative change rates (RCRs).

Across the full range of the intelligence distribution, we observed the following trends for cortical thickness (Figure 5, Left Panel): a) no changes until 10 years of age, b) statistically significant thinning for individuals with lower intelligence scores in early adolescence (10-14 years of age), and c) thinning for all individuals.

Regarding cortical surface area (Figure 5, Right Panel) we found a) expansion until 9 years of age, b) contraction at 11-12 years of age, especially for individuals with higher intelligence scores, and c) surface contraction through 16 years of age for individuals with lower intelligence scores. Nevertheless, surface area developmental changes were not statistically significant regarding the estimated intelligence differences.

4.3. Comparison with previous studies

Generalized cortical thinning in the period considered here has been observed before (Alemán-Gómez et al., 2013, Sowell et al., 2003, 2007, Zhou et al., 2015) and cortical surface area expansion has been appreciated in early adolescence (Schnack et al., 2014).

However, these developmental cortical changes cannot be simply generalized to individuals showing distinguishable intellectual levels. In this regard, the study by Shaw et al. (2006) reported cortical thickness changes related with intelligence levels: there was a negative correlation between thickness and intelligence differences in early childhood, whereas the correlation was positive in late childhood and early adolescence. Furthermore, brightest children showed greater plasticity along the considered time period.

The present study failed to find greatest plasticity in individuals showing higher intelligence levels, and therefore, Shaw et al.'s results were not replicated. Indeed, brightest individuals showed here remarkable cortical thickness preservation along the considered developmental period, whereas individuals with lower intelligence levels showed substantial thinning in early adolescence. Therefore, the present findings can be seen as consistent with those observed in the Burgaleta et al.'s (2014) study: a) individuals showing intelligence gains over time showed cortical thickness preservation, and b) individuals showing cortical thinning lost IQ points during the same period. They are also in coherence with Román et al.'s (2016) training research described above.

The Schnack et al.'s (2014) report underscored the interaction between intelligence differences assessed at baseline and cortical development, as described at the introduction section. Their findings revealed substantial thinning over time in less intelligent individuals, which is consistent with the results observed here. Regarding cortical surface area, they found that individuals with higher intelligence levels stop their cortical expansion at early ages than individuals with lower intelligence levels. The results observed in the present study revealed surface area contractions beginning at 11 years of age for all individuals, but this trend stops earlier in brighter individuals than in individuals with lower intelligence levels. Anyways, the findings support relative stability for cortical surface area across the time period considered.

4.4. Conclusion

The present research corroborates the complex nature of the brain-intelligence relationships across the period of the life span considered. We failed to substantiate the claim that brighter individuals show greater brain plasticity. This key finding is consistent

with results observed in the computational investigation reported by Thomas (2016) who asked: do more intelligent brains retain heightened plasticity for longer in development? The short answer was NO: “*the genetic influence on behavior via the neurocomputational properties remains relatively consistent across development*”.

Nevertheless, the findings reported here highlight remarkable cortical thinning for individuals with lower intelligence levels in early adolescence. This thinning process becomes visible in brighter individuals only in late adolescence. Furthermore, the observed cortical thinning last longer in individuals showing lower intelligence scores than in those with higher intelligence scores. Surface area contraction also last longer in individuals with lower intelligence scores, although this trend was not statistically significant.

The temporal and frontal lobes comprised regions manifesting developmental changes – in both cortical thickness and cortical surface area—related with individual differences in the general factor of intelligence (*g*). The findings support the conclusion that individual differences in general intelligence are related with brain structural changes. Brighter individuals show cortical thickness preservation and light thinning is observed for these individuals in late adolescence only. Individuals showing lower intelligence levels show greater thinning in early and late adolescence.

Finally, we acknowledge that the observed relationships cannot tell if intelligence modulates cortical changes or the other way around. Cross-lagged analyses may help to shed light regarding this crucial point (Watkins, Lei, & Canivez, 2007).

5. REFERENCES

- Ad-Dab'bagh, Y., Lyttelton, O., Muchlboeck, J. S., Lepage, C., Einarson, D., Mok, K. ... & Evans, A. C. (2006). The CIVET image-processing environment: a fully automated comprehensive pipeline for anatomical neuroimaging research. *In Proceedings of the 12th annual meeting of the organization for human brain mapping* (p. 2266).
- Alemán-Gómez, Y., Janssen, J., Schnack, H., Balaban, E., Pina-Camacho, L., Alfaro-Almagro, F., ... & Desco, M. (2013). The human cerebral cortex flattens during adolescence. *The Journal of Neuroscience*, 33, 15004-15010.
- Barbey, AK, Colom, R, Solomon, J., Krueger F, Forbes, C. & Grafman J. (2012). An integrative architecture for general intelligence and executive function revealed by lesion mapping. *Brain*, 135, 1154-1164.
- Basten, U., Hilger, K. & Fiebach, C. J. (2015). Where smart brains are different: A quantitative meta-analysis of functional and structural brain imaging studies on intelligence. *Intelligence*, 51, 10-27.
- Bentler, P. M. (1990). Comparative fit indexes in structural models. *Psychological Bulletin*, 107, 238-246. doi:10.1037/0033-2909.107.2.238
- Browne, M. W. & Cudeck, R. (1993). Alternative ways of assessing model fit. In K.A. Bollen, & J.S. Long (Eds.), *Testing Structural Equation Models* (pp 136-162). Newbury Park, CA: Sage.
- Burgaleta, M., Johnson, W., Waber, D. P., Colom, R., & Karama, S. (2014). Cognitive ability changes and dynamics of cortical thickness development in healthy children and adolescents. *NeuroImage*, 84, 810-819.

- Cleveland, W. S. & Devlin, S. J. (1988). Locally weighted regression: An approach to regression analysis by local fitting. *Journal of the American Statistical Association*, 83, 403, 596-610.
- Colom, R., Burgaleta, M., Román, F. J., Karama, S., Álvarez-Linera, J., Abad, F. J., ... & Haier, R. J. (2013). Neuroanatomic overlap between intelligence and cognitive factors: Morphometry methods provide support for the key role of the frontal lobes. *NeuroImage*, 72, 143-152.
- Colom, R., Haier, R.J., Head, K., Álvarez-Linera, J., Quiroga, M^aA., Shih, P.C. & Jung, R.E. (2009). Gray matter correlates of fluid, crystallized, and spatial intelligence: Testing the P-FIT model. *Intelligence*, 37, 124-135.
- Colom, R., Karama, S., Jung, R. E., & Haier, R. J. (2010). Human intelligence and brain networks. *Dialogues In Clinical Neuroscience*, 12, 489-501.
- Colom, R. & Thompson, P.M. (2011). Understanding Human Intelligence by Imaging the Brain. In T. Chamorro-Premuzic, S. von Stumm, & A. Furnham (Eds.), *Handbook of Individual Differences*. London: Wiley-Blackwell.
- Ducharme, S., Albaugh, M. D., Nguyen, T., Hudziak, J. J., Mateos-Pérez, J. M., Labbe, A., et al. (2016). Trajectories of cortical thickness maturation in normal brain development –The importance of quality control processes. *NeuroImage*, 125, 267-279.
- Estrada, E., Ferrer, E., Abad, F. J., Román, F. J., & Colom, R. (2015). A general factor of intelligence fails to account for changes in tests' scores after cognitive practice: A longitudinal multi-group latent-variable study. *Intelligence*, 50, 93-99.
- Evans, A. C., & Brain Development Cooperative Group (2006). The NIH MRI study of normal brain development. *NeuroImage*, 30, 184-202.

- Gläscher, J., Rudrauf, D., Colom, R., Paul, L.K., Tranel, D., Damasio, H. & Adolphs, R. (2010). The distributed neural system for general intelligence revealed by lesion mapping. *PNAS*, 107, 10, 4705-4709.
- Haier, R.J., Colom, R., Schroeder, D., Condon, C., Tang, C., Eaves, E. & Head, K. (2009). Gray matter and intelligence factors: Is there a neuro-g? *Intelligence*, 37, 136-144.
- Johnson, W. (2013). Whither Intelligence Research? *Journal of Intelligence*, 1, 25-35.
- Karama, S., Ad-Dab'bagh, Y., Haier, R. J., Deary, I., Lyttelton, ... & the Brain Development Cooperative Group (2009). Positive association between cognitive ability and cortical thickness in a representative US sample of healthy 6 to 18 year-olds. *Intelligence*. 37, 145-155.
- Kim, J. S., Singh, V., Lee, J. K., Lerch, J., Ad-Dab'bagh, Y., MacDonald, D. ... & Evans, A. C. (2005). Automated 3-D extraction and evaluation of the inner and outer cortical surfaces using a Laplacian map and partial volume effect classification. *NeuroImage*, 27, 210-221.
- Koenis, M. M. G., Brouwer, R. M., van den Heuvel, M. P., Mandl, R. C. W., van Soelen, I. L. C., Kahn, R. S., Boomsma, D. I., Hulshoff Pol, H. E. (2015). Development of the Brain's Structural Network Efficiency in Early Adolescence: A Longitudinal DTI Twin Study. *Human Brain Mapping*, 36, 12, 4938-4953.
- MacDonald, D., Kabani, N., Avis, D. & Evans, A. C. (2000). Automated 3-D extraction of inner and outer surfaces of cerebral cortex from MRI. *NeuroImage*, 12, 340-356.
- McArdle, J. J. (1988). Dynamic but Structural Equation Modeling of Repeated Measures Data. In J. R. Nesselroade & R. B. Cattell (Eds.), *Handbook of Multivariate Experimental Psychology* (2nd Ed. pp. 561-614). Springer US.

- Meredith, W. M. (1993). Measurement invariance, factor analysis, and factorial invariance. *Psychometrika*, 58, 525–543. doi:10.1007/BF02294825
- Meredith, W. & Horn, J. (2001). The role of factorial invariance in modeling growth and change. In L. M. Collins & A. G. Sayer (Eds.), *New methods for the analysis of change* (pp. 203–240). Washington, DC: American Psychological Association. doi:10.1037/10409-007
- Muthén, L.K. and Muthén, B.O. (1998, 2015). *Mplus User's Guide*. Seventh Edition. Los Angeles, CA: Muthén & Muthén.
- Román, F. J., Abad, F. J., Escorial, S., Burgaleta, M., Martínez, K., Álvarez-Linera, J., ... & Colom, R. (2014). Reversed hierarchy in the brain for general and specific cognitive abilities: A morphometric analysis. *Human Brain Mapping*, 35, 3805-3818.
- Román, F. J., Lewis, L. B., Chen, Chi-Hua, Karama, S., Burgaleta, M., Martínez, K., Lepage, C., Jaeggi, S. M., Evans, A. C., Kremen, W. S. & Colom, R. (2016). Gray matter responsiveness to adaptive working memory training: A Surface-Based Morphometry Study. *Brain Structure & Function*, 221, 4369-4382.
- Salthouse, T. A. (2017). Shared and unique influences on age-related cognitive change. *Neuropsychology*, 31, 1, 11-19.
- Schnack, H. G., van Haren, N. E., Brouwer, R. M., Evans, A., Durston, S., Boomsma, D. I., ... & Pol, H. E. H. (2014). Changes in thickness and surface area of the human cortex and their relationship with intelligence. *Cerebral Cortex*, 25, 6, 1608-1617.
- Schreiber, J. B., Nora, A., Stage, F. K., Barlow, E. A. & King, J. (2006). Reporting Structural Equation Modeling and Confirmatory Factor Analysis Results: A Review. *The Journal of Educational Research*, 99, 323-338. doi:10.3200/JOER.99.6.323-338

- Schweizer, K. (2010). Some Guidelines Concerning the Modeling of Traits and Abilities in Test Construction. *European Journal of Psychological Assessment*, 26, 1-2. doi:10.1027/1015-5759/a000001
- Shaw, P., Greenstein, D., Lerch, J., Clasen, L., Lenroot, R., Gogtay, N., ... & Giedd, J. (2006). Intellectual ability and cortical development in children and adolescents. *Nature*, 440, 676-679.
- Sowell, E. R., Peterson, B. S., Thompson, P. M., Welcome, S. E., Henkenius, A. L., & Toga, A. W. (2003). Mapping cortical change across the human life span. *Nature Neuroscience*, 6, 309-315.
- Sowell, E. R., Thompson, P. M., Leonard, C. M., Welcome, S. E., Kan, E. & Toga, A. W. (2004). Longitudinal mapping of cortical thickness and brain growth in normal children. *The Journal of Neuroscience*, 24, 38, 8223-8231.
- Sowell, E. R., Thompson, P. M. & Toga, A. W. (2007). Mapping adolescent brain maturation using structural magnetic resonance imaging. In D. Romer & E. F. Walker (Eds.), *Adolescent psychopathology and the developing brain: Integrating brain and prevention science*. Oxford University Press. DOI:10.1093/acprof:oso/9780195306255.003.0003
- Taki, Y., Hashizume, H., Sassa, Y., Takeuchi, H., Asano, M. Asano, K. et al. (2012). Correlation among body height, intelligence, and brain gray matter volume in healthy children. *NeuroImage*, 16, 59, 2, 1023-1027.
- Thomas, M. S. C. (2016). Do more intelligent brains retain heightened plasticity for longer in development? A computational investigation. *Developmental Cognitive Neuroscience*, 19, 258-269.
- Tucker, L. R. & Lewis, C. (1973). A reliability coefficient for maximum likelihood factor analysis. *Psychometrika*, 38, 1-10. doi:10.1007/BF02291170

- Van Petten, C. (2004). Relationship between hippocampal volume and memory ability in healthy individuals across the lifespan: Review and meta-analysis. *Neuropsychologia*, 42, 1394–1413.
- Watkins, M. W., Pui-Wa, L. & Canivez, G. L. (2007). Psychometric intelligence and achievement: A cross-lagged panel analysis. *Intelligence*, 35, 59-68.
- Wechsler, D. (1999). *Wechsler Abbreviated Scale of Intelligence*. Harcourt Brace and Company, San Antonio.
- Widaman, K. F., Ferrer, E. & Conger, R. D. (2010). Factorial Invariance Within Longitudinal Structural Equation Models: Measuring the Same Construct Across Time. *Child Development Perspectives*, 4, 10–18. doi:10.1111/j.1750-8606.2009.00110.x
- Widaman, K. F. & Reise, S. P. (1997). Exploring the measurement invariance of psychological instruments: Applications in the substance use domain. In K. J. Bryant, M. Windle & S. G. West, *The science of prevention: Methodological advances from alcohol and substance abuse research*. (pp. 281-324). Washington, DC: American Psychological Association.
- Wierenga, L. M., Langen, M., Oranje, B. & Durston, S. (2014). Unique developmental trajectories of cortical thickness and surface area. *NeuroImage*, 87, 120–126.
- Zhou, D., Lebel, C., Treit, S., Evans, A. & Beaulieu, C. (2015). Accelerated longitudinal cortical thinning in adolescence. *NeuroImage*, 104, 138-145.

FIGURE LEGENDS

Figure 1. Timeline of the present study

Figure 2. Structural equation model for estimating the general factor of intelligence (g) and studying factorial invariance across time points (t_1 , t_2 , t_3)

Figure 3. Left Panel: age changes in cortical thickness (CT), cortical surface area (CSA), and general intelligence (g). Each participant is represented as a trend line with a point standing for each of the three time measures (t_1 , t_2 , and t_3). Hot colors denote abrupt increases in intelligence (Δg). **Right Panel:** correlation between changes in g (horizontal axis, reversed) and changes in cortical thickness (CT) and cortical surface area (CSA) (vertical axis). Each individual is represented by one point, and the age of the first evaluation is represented by the color of these points.

Figure 4. Square effect ($\text{age}^2 \times g$ factor) found at the vertex level for cortical thickness (blue), cortical surface area (green) and both cortical indices (red).

Figure 5. Top Panel: Relative change rates (RCRs) in cortical thickness (CT) and cortical surface area (CSA) over time for the different levels of g (general cognitive ability). Results for CT reveal prolonged thinning for less intelligence individuals (from 10 to 18 years of age), whereas this thinning process becomes visible only in late adolescence (17 years) for more intelligence individuals. Therefore, brighter individuals show prolonged thickness preservation. Results for CSA show great expansion in childhood for all individuals regardless of their intellectual levels. Surface contraction is revealed at 11 years of age, especially for brighter individuals. This contraction process continues for a longer period of time in less intelligent individuals. **Bottom Panel:** Statistically significant differences were found for cortical thickness in the period ranging from 10 to 14 years of age: individuals with lower intelligence scores show substantial thinning, whereas brighter individuals show cortical thickness preservation.

Acknowledgment. We thank Hugo Schnack for their help with the *Relative Change Rate* (*RCR*) computations applied to the present dataset.

Table 1
Nested model comparison across time

Parameter	Model 1 Conf. Inv	Model 2a Weak FI	Model 2b Weak Partial FI(*)	Model 3 Strong FI	Model 4 Strict FI	Model 5 Strict FI, constant loadings (age -> g) across time
n of Parameters	54	46	48	44	38	36
ChiSq	122.4	173.0	140.8	148.9	165.1	301.7
df	72	80	78	82	88	90
ChiSq / df	1.7	2.2	1.8	1.8	1.9	3.4
Increase ChiSq		50.6	18.4	8.1	16.2	136.6
Increase df		8	6	4	6	2
CFI	.975	.955	.969	.967	.962	.897
TLI	.965	.942	.960	.959	.956	.883
RMSEA	.073	.094	.078	.078	.081	.133
RMSEA_90CI_Lower	.050	.074	.057	.058	.062	.117
RMSEA_90CI_Upper	.094	.113	.098	.098	.100	.150

(*) Matrix reasoning test was freely estimated across time.

Table 2

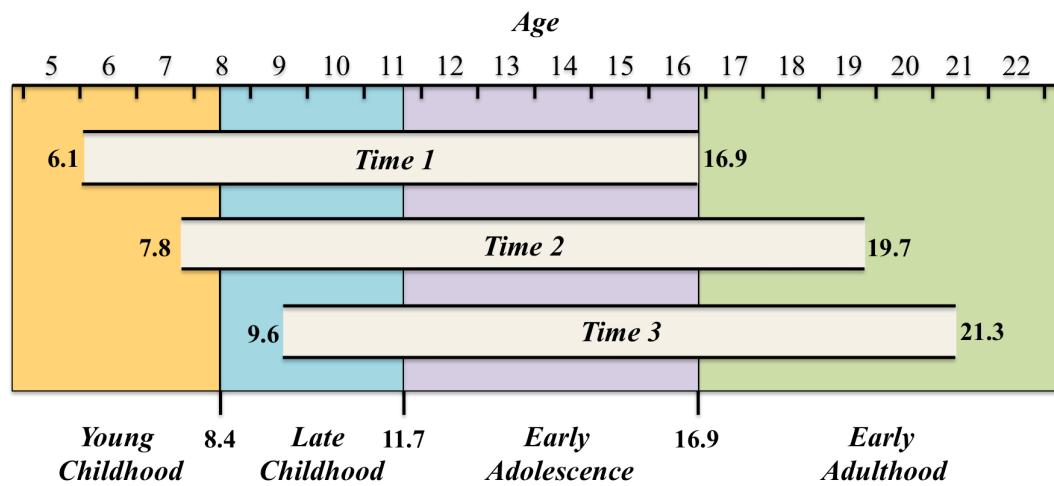
Wald's Tests for pair comparisons of the regression loadings (Age \rightarrow g) across time

	<i>Wald's statistic</i>	<i>df</i>	<i>p</i>
H0: $t1 = t2$	53.294	1	< .0001
H0: $t2 = t3$	54.341	1	< .0001
H0: $t1 = t3$	104.31	1	< .0001

Table 3

Mean values for g across time ($t1$, $t2$, and $t3$). Time (t) and effect size (d)

g	$t1$	$t2$	$t3$	Change $t2-t1$	Change $t3-t2$	Change $t3-t1$
Mean	6.78	8.08	8.92	1.30 ($d = .60$)	0.84 ($d = .48$)	2.14 ($d = .98$)
SD	2.17	1.74	1.38			



N = 132 x 3 times = 396 registers

FIGURE 1

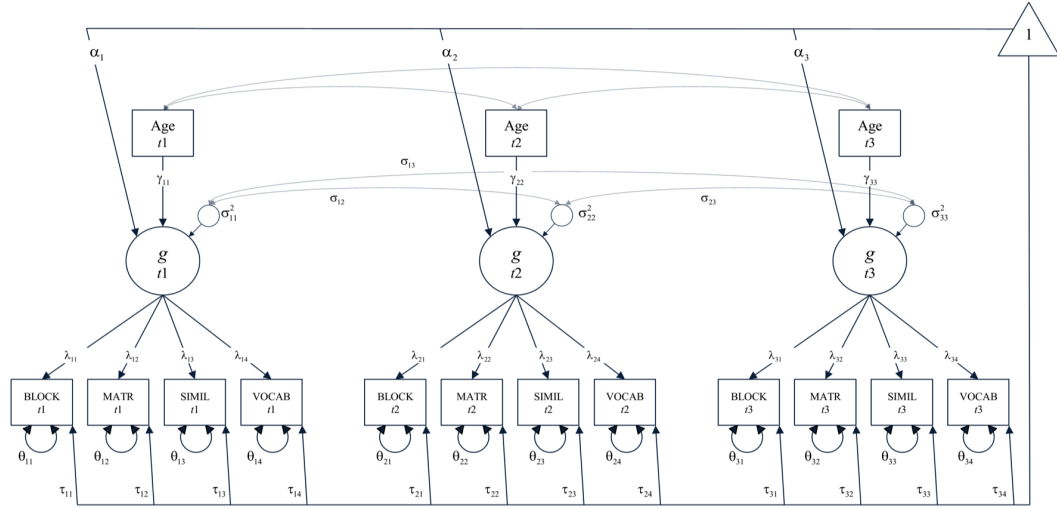


FIGURE 2

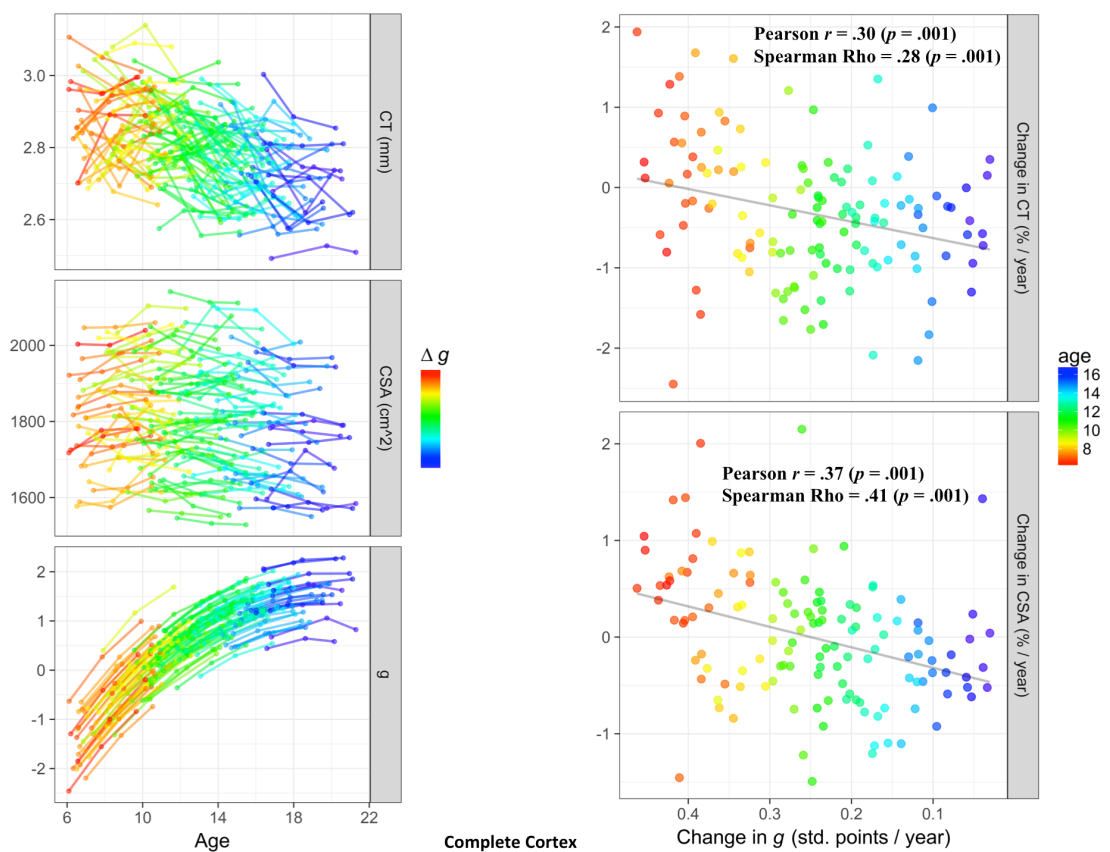


FIGURE 3

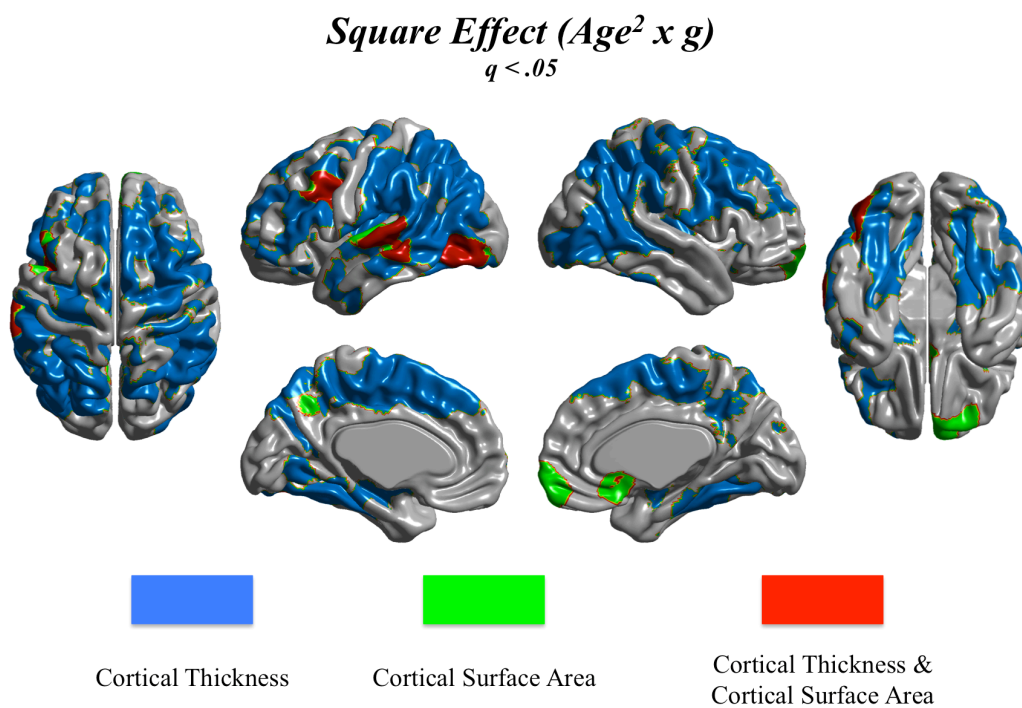


FIGURE 4

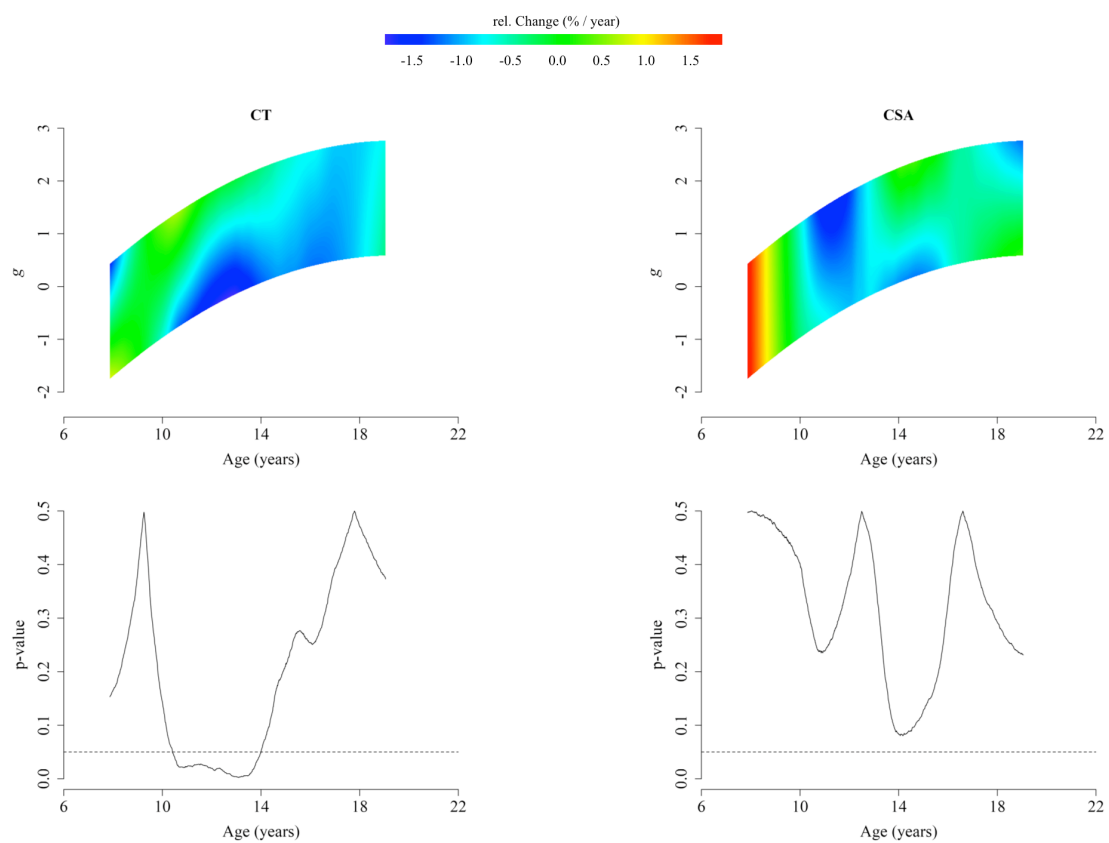


FIGURE 5